Characterization of Five-Coordinate Ruthenium(II) Phosphine Complexes by X-ray Diffraction and Solid-State ^{31}P CP/MAS NMR Studies and Their Reactivity with Sulfoxides and Thioethers

Kenneth S. MacFarlane, Ajey M. Joshi, Steven J. Rettig, and Brian R. James*

Department of Chemistry, The University of British Columbia, Vancouver, BC V6T 1Z1, Canada

Received July 18, 1996[⊗]

^{31}P CP/MAS NMR spectroscopy is examined as a method of characterization for ruthenium(II) phosphine complexes in the solid state, and the results are compared with X-ray crystallographic data determined for $RuCl_2$(dppb)(PPh_3) (dppb = $Ph_2P(CH_2)_4PPh_2$), $RuBr_2(PPh_3)_3$, and the previously determined $RuCl_2(PPh_3)_3$. Crystals of $RuBr_2(PPh_3)_3$ ($C_{54}H_{45}Br_2P_3Ru$) are monoclinic, space group $P2_1/a$, with $a = 12.482(4)$ Å, $b = 20.206(6)$ Å, $c = 17.956(3)$ Å, $\beta = 90.40(2)°$, and $Z = 4$, and those of $RuCl_2$(dppb)(PPh_3) ($C_{46}H_{43}Cl_2P_3Ru$) are also monoclinic, space group $P2_1/n$, with $a = 10.885(2)$ Å, $b = 20.477(1)$ Å, $c = 18.292(2)$ Å, $\beta = 99.979(9)°$, and $Z = 4$. The structure of $RuBr_2(PPh_3)_3$ was solved by direct methods, and that of $RuCl_2$(dppb)(PPh_3) was solved by the Patterson method. The structures were refined by full-matrix least-squares procedures to $R = 0.048$ and 0.031 ($R_w = 0.046$ and 0.032) for 5069 and 5925 reflections with $I \geq 3\sigma(I)$, respectively. Synthetic routes to $RuBr_2$(dppb)(PPh_3) and [RuBr(dppb)]$_2$(μ_2-dppb) are reported. The reactivity of $RuCl_2$(dppb)(PPh_3) with the neutral two-electron donor ligands (L) dimethyl sulfoxide, tetramethylene sulfoxide, tetrahydrothiophene, and dimethyl sulfide to give [(L)(dppb)Ru(μ-Cl)$_3$RuCl(dppb)] is discussed.

Introduction

Work from this laboratory has investigated the ability of chlororuthenium complexes containing a single, chelating ditertiary phosphine (P−P) per Ru atom to catalyze the hydrogenation of unsaturated organics, including imines.[1] We are interested in extending these studies to the bromoruthenium analogs, and therefore the development of synthetic routes to these species was necessary. The synthetic methodology used in this laboratory previously to prepare [RuCl(P−P)]$_2$(μ-Cl)$_2$ complexes consisted of the H_2 reduction of the mixed-valence, triply-chloro-bridged complexes [RuCl(P−P)]$_2$(μ-Cl)$_3$ which were themselves prepared by the reaction of 1 equiv of P−P ligand with $RuCl_3(PR_3)_2$(DMA)·DMA solvate, where DMA = *N*,*N*-dimethylacetamide and R = Ph or *p*-tolyl.[2] The obvious entry into the bromoruthenium analogs therefore was from the known $RuBr_3(PR_3)_2$ complex.[3] Unfortunately, this complex could not be prepared pure. Dekleva of this laboratory has noted difficulties in isolating this complex,[4] the problems being similar to those encountered in the preparation of $RuCl_3(PPh_3)_2$(MeOH).[5,6] Therefore, another route to the bromo dinuclear diphosphine complexes was necessary. The complex $RuCl_2$(dppb)(PPh_3), which is readily prepared from $RuCl_2(PPh_3)_3$, is known in solution to be in equilibrium with dinuclear [RuCl(dppb)]$_2$(μ-Cl)$_2$ (see eq 1).[2,7] Therefore, if the bromo analog

$$2RuCl_2(dppb)(PPh_3) \rightleftharpoons [RuCl(dppb)]_2(\mu\text{-}Cl)_2 + 2PPh_3 \quad (1)$$

$RuBr_2$(dppb)(PPh_3) could be prepared, a corresponding equilibrium dissociation could allow for isolation of [RuBr(dppb)]$_2$(μ-Br)$_2$. The geometry of the five-coordinate complex $RuCl_2$(dppb)(PPh_3) has previously been suggested to be square pyramidal by low-temperature ^{31}P{^{1}H} NMR spectroscopic studies.[7]

We were also interested in establishing routes from $RuCl_2$(dppb)(PPh_3) to triply-chloro-bridged diruthenium(II,II) species as well as investigating the utility of solid-state ^{31}P CP/MAS NMR spectroscopy for the characterization of the five-coordinate Ru species; [RuCl(dppb)]$_2$(μ-Cl)$_2$ species are known to react generally with a ligand L to generate (L)(dppb)Ru(μ-Cl)$_3$RuCl(dppb).[2] The species with L = dmso, where dmso implies *S*-bonded sulfoxide, has previously been prepared in this laboratory from *cis*-$RuCl_2(dmso)_4$ and studied by X-ray diffraction and ^{31}P{^{1}H} NMR spectroscopy;[2] therefore, the reactivity of dmso with $RuCl_2$(dppb)(PPh_3) was a good starting point as one of the possible products [(dmso)(dppb)Ru(μ-Cl)$_3$RuCl(dppb)] had been characterized previously.

In this paper, we report the results of ^{31}P CP/MAS NMR spectroscopic studies on $RuCl_2(PPh_3)_3$ and $RuCl_2$(dppb)(PPh_3) as well as X-ray crystallographic studies of $RuBr_2(PPh_3)_3$ and $RuCl_2$(dppb)(PPh_3). Details of synthetic chemistry using $RuCl_2$(dppb)(PPh_3) as a precursor and the characterization of the products [(L)(dppb)Ru(μ-Cl)$_3$RuCl(dppb)] by solution ^{31}P{^{1}H} NMR spectroscopy are reported.

Experimental Section

General Procedures and Materials. Manipulations were carried out under Ar using standard Schlenk techniques. Reagent grade solvents (Fisher Scientific) were distilled from CaH_2 (CH_2Cl_2), sodium (diethyl ether, C_6H_6 and hexanes), or Mg/I_2 (MeOH and EtOH) under N_2. Dibromomethane (Aldrich) was dried over molecular sieves (4 Å) prior to use. Dimethyl sulfoxide (dmso), tetramethylene sulfoxide (tmso), dimethyl sulfide (dms), and tetrahydrothiophene (tht) were used as received from Aldrich. 1,4-Bis(diphenylphosphino)butane (dppb)

[⊗] Abstract published in *Advance ACS Abstracts,* November 1, 1996.

(1) Fogg, D. E.; James, B. R.; Kilner, M. *Inorg. Chim. Acta* **1994**, *222*, 85.
(2) Joshi, A. M.; Thorburn, I. S.; Rettig, S. J.; James, B. R. *Inorg. Chim. Acta* **1992**, *198*, 283.
(3) Stephenson, T. A.; Wilkinson, G. *J. Inorg. Nucl. Chem.* **1966**, *28*, 945.
(4) Dekleva, T. W. Ph.D. Thesis, The University of British Columbia, 1983.
(5) Ruiz-Ramirez, L.; Stephenson, T. A.; Switkes, E. S. *J. Chem. Soc., Dalton Trans.* **1973**, 1770.
(6) Pez, G. P.; Grey, R. A.; Corsi, J. *J. Am. Chem. Soc.* **1981**, *103*, 7528.
(7) Jung, C. W.; Garrou, P. E.; Hoffman, P. R.; Caulton, K. G. *Inorg. Chem.* **1984**, *23*, 726.

S0020-1669(96)00860-9 CCC: $12.00

was used as supplied by Aldrich. 1,4-Bis(dicyclohexylphosphino)-butane (dcypb) was prepared[8] by a modified reported procedure from dicyclohexylphosphine, ^{n}BuLi, and 1,4-dibromobutane.[9] $RuCl_2(PPh_3)_3$ (**1**),[3,10] $RuBr_2(PPh_3)_3$ (**2**),[3,4,11] $RuCl_2(P(p\text{-tolyl})_3)_3$ (**3**),[4,12,13] and $RuCl_2$-(dppb)(PPh_3) (**4**)[2,7] were prepared according to published procedures. Solution NMR spectra were recorded on a Varian XL300 spectrometer (121.42 MHz for $^{31}P\{^1H\}$), using residual solvent proton (^1H) or external $P(OMe)_3$ ($^{31}P\{^1H\}$: δ 141.00 vs external 85% aqueous H_3PO_4) as the reference. The $^{31}P\{^1H\}$ solid-state cross polarization, magic-angle spinning (CP/MAS) FT-NMR spectra were recorded (with the kind help of Dr. A. Root formerly of this department) on a Bruker MSL400 or a Bruker CPX200 instrument (161.97 and 80.99 MHz for ^{31}P, respectively). All ^{31}P chemical shifts (solid state and solution) are reported with respect to external 85% aqueous H_3PO_4. The samples were packed as powders (~0.2−0.3 g) in Teflon holders of ~8 mm i.d. High-resolution, solid-state ^{31}P NMR spectra were obtained, by combining high-power proton decoupling with $^1H-^{31}P$ cross polarization (CP) (5.5 μs 90° *y* ^1H pulse, 1 ms contact time, 1 s recycle time) and magic-angle spinning (MAS) at ~2.5−4.0 kHz. The solution and solid-state $^{31}P\{^1H\}$ NMR data for the complexes are given in the Results and Discussion section (Tables 3−5). The ^1H NMR data are presented in this Experimental Section for purposes of characterization; the data are straightforward and are not discussed. The UV−vis spectra were recorded on a Hewlett Packard 8452A diode array spectrophotometer and are given as λ_{max} (nm) [ϵ_{max} (M^{-1} cm^{-1})], sh = shoulder. IR spectra (Nujol mulls, KBr plates) were recorded (cm^{-1}) on an ATI Mattson Genesis FTIR spectrometer (s = strong). Elemental analyses were performed by Mr. P. Borda of this department.

$RuCl_2$(dppb)(PPh_3), 4. Crystals of **4** were isolated as green plates from a toluene-d_8 solution of **4** and 14 equiv of PPh_3 after several months in a N_2 glovebox.

$RuCl_2$(dppb)$(P(p\text{-tolyl})_3)$, 5. The title complex was prepared in much the same manner as for the PPh_3 analog **4**.[2] Complex **3** (1.0 g, 0.92 mmol) was dissolved in CH_2Cl_2 (20 mL), then dppb (0.39 g, 0.92 mmol) was added under a flow of Ar, and the reaction mixture was stirred at room temperature (rt) for 2 h. The initially orange solution changed to dark green upon addition of the phosphine. On occasion, some bridged-phosphine complex, $[RuCl_2(dppb)]_2(\mu$-dppb), was present.[2,7] This insoluble green complex was removed by vacuum filtration (0.08 g, ~10% of the Ru). The green filtrate was then reduced to ~5 mL, and EtOH (40 mL) was added to precipitate the green product, which was isolated by filtration, washed with EtOH (2 × 10 mL) and hexanes (3 × 10 mL), and dried under vacuum. Yield: 0.83 g (76%). ^1H NMR (300 MHz, C_6D_6, 20 °C): δ 1.38 (br m, 4H, PCH_2CH_2 of dppb), 2.02 (s, 9H, C*H*$_3$ of *p*-tolyl), 2.92 (br m, 4H, PC*H*$_2$ of dppb), 6.65−7.95 (m, 32H, 20H of Ph of dppb and 12H of Ph of $P(p\text{-tolyl})_3$). Anal. Calcd for $C_{49}H_{49}Cl_2P_3Ru$: C, 65.19; H, 5.47; Cl, 7.85. Found: C, 64.91; H, 5.36; Cl, 7.65.

$RuBr_2$(dppb)(PPh_3), 6. This bromo analog was prepared in much the same manner as the chloro derivative **5**, the only difference being that the reaction was performed in CH_2Br_2. Complex **2** (0.52 g, 0.49 mmol) and dppb (0.20 g, 0.48 mmol) were dissolved in CH_2Br_2 (10 mL), and the mixture was stirred for 2 h at rt when the originally deep-red solution gradually changed to yellow-orange. The reaction mixture was reduced to ~5 mL and EtOH (40 mL) was added to precipitate the product. An olive solid was collected, washed with EtOH (2 × 10 mL) and hexanes (2 × 10 mL), and finally dried under vacuum. Yield: 0.45 g (97%). Anal. Calcd for $C_{46}H_{43}Br_2P_3Ru$: C, 58.18; H, 4.56; Br, 16.83. Found: C, 58.04; H, 4.64; Br, 16.76. Crystals of the starting material $RuBr_2(PPh_3)_3$ were isolated from the filtrate of the above preparation as dark-orange prisms.

[(dppb)$Br_2Ru(\mu_2$-(dppb))$RuBr_2$(dppb)], 7a. Complex **2** (0.10 g, 0.095 mmol) was stirred with 2 equiv of dppb (0.081 g, 0.19 mmol) in C_6H_6 (25 mL) for 1 h at rt under Ar. The resulting green solution was reduced in volume to ~5 mL, and hexanes (20 mL) was added to precipitate a mustard solid. The mustard product was collected by filtration, washed with hexanes (4 × 10 mL), and dried under vacuum. The diphosphine-bridged complexes (**7a**,**b**), occasionally isolated as a side product in the preparation of $RuX_2(P-P)(PAr_3)$ species, are essentially insoluble in most nonaromatic solvents and only sparingly soluble in aromatic solvents; their insolubility prevented the measurement of NMR spectra. Yield: 0.053 g (61%). UV−vis (C_6H_6): 364 [2580], 466 [3620], 710 [1170]. Anal. Calcd for $C_{84}H_{84}Br_4P_6Ru_2$: C, 56.01; H, 4.70; Br, 17.74. Found: C, 56.27; H, 4.58; Br, 17.52.

[(dcypb)$Cl_2Ru(\mu_2$-(dcypb))$RuCl_2$(dcypb)], 7b. The general procedure outlined for **7a** was followed but using **1** (0.18 g, 0.19 mmol) and dcypb (0.18 g, 0.40 mmol). Yield of the green solid: 0.13 g (77%). UV−vis (C_6H_6): 340 [5080], 384 (sh) [3870], 682 [1940]. Anal. Calcd for $C_{84}H_{156}Cl_4P_6Ru_2$: C, 59.49; H, 9.27; Cl, 8.36. Found: C, 59.40; H, 9.33; Cl, 8.08.

[(dmso)(dppb)Ru(μ-Cl)$_3$RuCl(dppb)], 8. An excess of dmso (170 μL, 2.3 mmol) was added to a dark-green suspension of **4** (0.18 g, 0.21 mmol) in C_6H_6 (5 mL). The originally green mixture became bright orange after refluxing for 1 h under Ar. The solution was cooled and hexanes (30 mL) added to precipitate a yellow-orange solid, which was collected on a sintered glass filter, washed with hexanes (5 × 5 mL) to remove PPh_3, and dried under vacuum. Yield: 0.12 g (87%). IR: $\nu_{S=O}$ 1090 (s, *S*-bonded dmso). ^1H NMR (300 MHz, $CDCl_3$, 20 °C): δ 0.65−2.32 (m, 21H, 15H of C*H*$_2$ of dppb and 6H of C*H*$_3$ of dmso), 3.50 (br m, 1H, C*H* of CH_2 dppb), 6.78 (m, 3H, Ph of dppb), 6.94−7.96 (m, 34H, Ph of dppb), 8.47 (m, 3H, Ph of dppb). ^1H NMR (300 MHz, C_6D_6, 20 °C): δ 0.50−2.50 (m, 16H, 10H of C*H*$_2$ of dppb and 6H of C*H*$_3$ of dmso), 2.74 (m, 1H, C*H* of CH_2 dppb), 3.29 (m, 3H, C*H*$_2$ dppb), 3.51 (m, 2H, C*H*$_2$ of dppb), 6.67 (t, 4H, Ph of dppb, J = 6.9 Hz), 6.80 (m, 16H, Ph of dppb), 7.34 (t, 3H, Ph of dppb, J = 8.3 Hz), 7.47 (br m, 5H, Ph of dppb), 7.61 (t, 2H, Ph of dppb, J = 6.8 Hz), 7.74 (t, 2H, Ph of dppb, J = 8.0 Hz), 8.07 (pseudo q, 4H, Ph of dppb, J = 8.9 Hz), 8.18 (t, 2H, Ph of dppb, J = 8.3 Hz), 8.67 (t, 2H, Ph of dppb, J = 8.0 Hz). UV−vis (C_6H_6): 378 [3010], 470 (sh) [590]; (CH_2Cl_2): 376 [2900], 470 (sh) [650]. Anal. Calcd for $C_{58}H_{62}Cl_4OP_4Ru_2S$: C, 54.64; H, 4.90. Found: C, 54.45; H, 5.10. This compound has been prepared previously from *cis*-$RuCl_2(dmso)_4$.[2] The above IR and $^{31}P\{^1H\}$ NMR spectroscopic data (see Table 5 below) agree with those reported in the literature,[2] while the UV−vis and ^1H NMR data have not been reported before.

[(tmso)(dppb)Ru(μ-Cl)$_3$RuCl(dppb)], 9. The complex was synthesized in the same manner as the dmso analog **8**. An excess of tmso (210 μL, 2.32 mmol) was added to a dark-green suspension of **4** (0.190 g, 0.221 mmol) in C_6H_6 (5 mL). The originally green mixture became bright orange after refluxing for 1.5 h under Ar. The solution was cooled and hexanes (30 mL) added to precipitate a pale-orange solid, which was collected on a sintered glass filter, washed with hexanes (5 × 5 mL) to remove PPh_3, and dried under vacuum. Yield: 0.11 g (70%). IR: $\nu_{S=O}$ 1093 (s, *S*-bonded tmso). ^1H NMR (300 MHz, $CDCl_3$, 20 °C): δ 0.65−3.10 (m, 20H, 12H of C*H*$_2$ of dppb and 8H of C*H*$_2$ of tmso), 3.26 (br m, 3H, C*H*$_2$ dppb), 3.73 (br m, 1H, C*H* of CH_2 dppb), 6.61 (br m, 3H, Ph of dppb), 7.00−8.12 (m, 35H, Ph of dppb), 8.51 (br m, 2H, Ph of dppb). ^1H NMR (300 MHz, C_6D_6, 20 °C): δ 0.30 (m, 23H, 15H of C*H*$_2$ of dppb and 8H of C*H*$_2$ of tmso), 3.82 (br m, 1H, C*H* of CH_2 dppb), 6.6−8.48 (m, 39H, Ph of dppb), 8.74 (br m, 1H, Ph of dppb). UV−vis (C_6H_6): 376 [2470], 460 (sh) [830]; (CH_2Cl_2): 374 [2410], 460 (sh) [600]. Anal. Calcd for $C_{60}H_{64}Cl_4OP_4Ru_2S$: C, 55.39; H, 4.96; Cl, 10.90; S, 2.46. Found: C, 55.11; H, 5.20; Cl, 10.71; S, 2.60.

[(dms)(dppb)Ru(μ-Cl)$_3$RuCl(dppb)], 10. An excess of dms (106 μL, 1.44 mmol) was added to a dark-green suspension of **4** (0.17 g, 0.20 mmol) in C_6H_6 (5 mL). The resulting mixture was stirred at rt (in a sealed Schlenk tube because of the smell and volatility of dms) under Ar for 4 h; the syntheses of the other sulfide and sulfoxide analogs were performed at reflux temperatures under a slow flow of Ar. An orange-brown product, precipitated by the addition of hexanes (30 mL), was collected by filtration, washed with hexanes (5 × 5 mL), and dried under vacuum. Yield: 0.11 g (87%). ^1H NMR (300 MHz, $CDCl_3$, 20 °C): δ 0.82−2.75 (m, 20H, 14H of C*H*$_2$ of dppb and 6H of C*H*$_3$ of dms), 3.13 (m, 1H, C*H* of CH_2 dppb), 3.70 (br m, 1H, C*H* of CH_2

(8) Chau, D. E. K.-Y. M.Sc. Thesis, The University of British Columbia, 1992.
(9) Priemer, H. Ph.D. Thesis, der Ruhr-Universität Bochum, 1987.
(10) Hallman, P. S.; Stephenson, T. A.; Wilkinson, G. *Inorg. Synth.* **1970**, *12*, 237.
(11) Wang, D. K. W. Ph.D. Thesis, The University of British Columbia, 1978.
(12) Knoth, W. H. *J. Am. Chem. Soc.* **1972**, *94*, 104.
(13) Armit, P. W.; Sime, W. J.; Stephenson, T. A.; Scott, L. *J. Organomet. Chem.* **1978**, *161*, 391.

Table 1. Crystallographic Data

compd	$RuBr_2(PPh_3)_3$ (**2**)	$RuCl_2(dppb)(PPh_3)$ (**4**)
formula	$C_{54}H_{45}Br_2P_3Ru$	$C_{46}H_{43}Cl_2P_3Ru$
fw	1047.75	860.74
cryst system	monoclinic	monoclinic
space group	$P2_1/a$	$P2_1/n$
a, Å	12.482(4)	10.885(2)
b, Å	20.206(6)	20.477(1)
c, Å	17.956(3)	18.292(2)
β, deg	90.40(2)	99.979(9)
V, Å^3	4528(1)	4015.8(6)
Z	4	4
ρ_{calc}, g/cm^3	1.537	1.424
ρ_{obsd}, g/cm^3	not measured	not measured
T, °C	21	21
radiation	Mo	Cu
λ, Å	0.710 69	1.541 78
μ, cm^{-1}	22.59	57.60
transm factors (relative)	0.73−1.00	0.55−1.00
$R(F)^a$	0.048	0.031
$R_w(F)^a$	0.046	0.032

^{a} $R = \sum||F_o| - |F_c||/\sum|F_o|$; $R_w = (\sum w(|F_o| - |F_c|)^2/\sum w|F_o|^2)^{1/2}$.

dppb), 6.65−7.80 (m, 35H, Ph of dppb), 8.04 (t, 2H, Ph of dppb, J = 7.8), 8.33 (m, 3H, Ph of dppb). ^{1}H NMR (300 MHz, C_6D_6, 20 °C): δ 0.52−2.75 (m, 20H, 14H of CH_2 of dppb and 6H of CH_3 of dms), 3.35 (br m, 1H, CH of CH_2 dppb), 4.12 (br m, 1H, CH of CH_2 dppb), 6.68−7.85 (m, 32H, Ph of dppb), 8.15 (m, 4H, Ph of dppb), 8.70 (m, 4H, Ph of dppb). UV−vis (C_6H_6): 374 [3780], 460 (sh) [730]; (CH_2Cl_2): 372 [3470], 460 (sh) [660]. Anal. Calcd for $C_{58}H_{62}Cl_4P_4Ru_2S$: C, 55.33; H, 4.96; Cl, 11.26; S, 2.55. Found: C, 55.48; H, 4.88; Cl, 11.11; S, 2.57.

[(tht)(dppb)Ru(μ-Cl)$_3$RuCl(dppb)], 11. The title product was synthesized in the same manner as the dmso analog **8**. An excess of tht (180 μL, 2.0 mmol) was added to a dark-green suspension of **4** (0.18 g, 0.21 mmol) in C_6H_6 (5 mL). The originally green mixture became bright orange after refluxing for 1 h under Ar. The solution was cooled and hexanes (30 mL) added to precipitate an orange-brown solid, which was collected on a sintered glass filter, washed with hexanes (5 × 5 mL) to remove PPh_3, and dried under vacuum. Yield: 0.12 g (90%). ^{1}H NMR (300 MHz, $CDCl_3$, 20 °C): δ 0.85−2.90 (m, 22H, 14H of CH_2 of dppb and 8H of CH_2 of tht), 3.20 (br m, 1H, CH of CH_2 dppb), 3.69 (br m, 1H, CH of CH_2 dppb), 6.78−7.75 (m, 35H, Ph of dppb), 8.07 (t, 2H, Ph of dppb, J = 8.8), 8.30 (m, 3H, Ph of dppb). ^{1}H NMR (300 MHz, C_6D_6, 20 °C): δ 0.50−2.75 (m, 22H, 14H of CH_2 of dppb and 8H of CH_2 of tht), 3.39 (br m, 1H, CH of CH_2 dppb), 4.10 (br m, 1H, CH of CH_2 dppb), 6.72−7.80 (m, 32H, Ph of dppb), 8.20 (br m, 4H, Ph of dppb), 8.65 (br m, 4H, Ph of dppb). UV−vis (C_6H_6): 374 [3700], 460 (sh) [605]; (CH_2Cl_2): 372 [3200], 460 (sh) [440]. Anal. Calcd for $C_{60}H_{64}Cl_4P_4Ru_2S$: C, 56.08; H, 5.02. Found: C, 56.61; H, 5.13. The slightly high C elemental analysis did not improve upon reprecipitation of the material.

X-ray Crystallographic Analyses of $RuBr_2(PPh_3)_3$ (2) and $RuCl_2$-(dppb)(PPh_3) (4). Selected crystallographic data appear in Table 1. The final unit-cell parameters were obtained by least-squares on the setting angles for 25 reflections with 2θ = 22.7−40.3° for **2** and 50.1−63.6° for **4**. The intensities of three standard reflections, measured every 200 reflections throughout the data collections, remained constant for both complexes. The data were processed[14] and corrected for Lorentz and polarization effects and absorption (empirical, based on azimuthal scans).

The structure of **2** was solved by direct methods, and that of **4** was solved by the Patterson method. All non-hydrogen atoms of both structures were refined with anisotropic thermal parameters. Hydrogen atoms were fixed in calculated positions (C−H = 0.99 Å for **2** and 0.98 Å for **4**, $B_H = 1.2B_{bonded\ atom}$). A secondary extinction correction (Zachariasen type, isotropic) was applied for **2**, the final value of the extinction coefficient being 1.3(1) × 10^{-7}. No extinction correction was necessary for **4**. Neutral atom scattering factors for all atoms[15] and anomalous dispersion corrections for the non-hydrogen atoms[16] were taken from the *International Tables for X-Ray Crystallography*. Selected bond lengths and bond angles appear in Table 2. A complete table of atomic coordinates and equivalent isotropic thermal parameters, crystallographic data, hydrogen atom parameters, anisotropic thermal parameters, bond lengths, bond angles, torsion angles, intermolecular contacts, and least-squares planes for both structures are included as Supporting Information.

Table 2. Selected Bond Lengths (Å) and Angles (deg) (Esd's in Parentheses)

$RuBr_2(PPh_3)_3$ (**2**)

Ru(1)−Br(1)	2.515(1)	Ru(1)−P(2)	2.389(2)
Ru(1)−Br(2)	2.526(1)	Ru(1)−P(3)	2.228(2)
Ru(1)−P(1)	2.423(2)	P−C	1.834(7)−1.857(7)

Br(1)−Ru(1)−Br(2)	155.64(4)	C(1)−P(1)−C(13)	106.9(3)
Br(1)−Ru(1)−P(1)	82.19(5)	C(7)−P(1)−C(13)	103.0(3)
Br(1)−Ru(1)−P(2)	84.31(5)	Ru(1)−P(2)−C(19)	117.4(2)
Br(1)−Ru(1)−P(3)	110.39(5)	Ru(1)−P(2)−C(25)	128.9(3)
Br(2)−Ru(1)−P(1)	93.04(5)	Ru(1)−P(2)−C(31)	100.1(2)
Br(2)−Ru(1)−P(2)	91.34(5)	C(19)−P(2)−C(25)	101.7(3)
Br(2)−Ru(1)−P(3)	93.96(5)	C(19)−P(2)−C(31)	104.7(3)
P(1)−Ru(1)−P(2)	156.43(7)	C(25)−P(2)−C(31)	100.4(3)
P(1)−Ru(1)−P(3)	101.28(7)	Ru(1)−P(3)−C(37)	114.1(2)
P(2)−Ru(1)−P(3)	101.50(7)	Ru(1)−P(3)−C(43)	119.7(2)
Ru(1)−P(1)−C(1)	104.4(2)	Ru(1)−P(3)−C(49)	117.2(2)
Ru(1)−P(1)−C(7)	128.5(2)	C(37)−P(3)−C(43)	100.0(3)
Ru(1)−P(1)−C(13)	115.3(2)	C(37)−P(3)−C(49)	101.6(3)
C(1)−P(1)−C(7)	95.4(3)	C(43)−P(3)−C(49)	101.5(3)

$RuCl_2(dppb)(PPh_3)$ (**4**)

Ru(1)−Cl(1)	2.3796(8)	Ru(1)−P(2)	2.2029(9)
Ru(1)−Cl(2)	2.4047(9)	Ru(1)−P(3)	2.3786(9)
Ru(1)−P(1)	2.3346(9)	P−C	1.820(4)−1.849(3)

Cl(1)−Ru(1)−Cl(2)	158.75(3)	Ru(1)−P(2)−C(4)	112.8(1)
Cl(1)−Ru(1)−P(1)	88.61(3)	Ru(1)−P(2)−C(17)	118.2(1)
Cl(1)−Ru(1)−P(2)	109.76(3)	Ru(1)−P(2)−C(23)	119.7(1)
Cl(1)−Ru(1)−P(3)	85.82(3)	C(4)−P(2)−C(17)	99.9(2)
Cl(2)−Ru(1)−P(1)	87.06(3)	C(4)−P(2)−C(23)	102.6(2)
Cl(2)−Ru(1)−P(2)	91.42(3)	C(17)−P(2)−C(23)	100.7(2)
Cl(2)−Ru(1)−P(3)	91.87(3)	Ru(1)−P(3)−C(29)	105.3(1)
P(1)−Ru(1)−P(2)	97.01(3)	Ru(1)−P(3)−C(35)	125.0(1)
P(1)−Ru(1)−P(3)	161.78(3)	Ru(1)−P(3)−C(41)	115.4(1)
P(2)−Ru(1)−P(3)	101.20(3)	C(29)−P(3)−C(35)	99.3(2)
Ru(1)−P(1)−C(1)	119.7(1)	C(29)−P(3)−C(41)	104.6(2)
Ru(1)−P(1)−C(5)	101.3(1)	C(35)−P(3)−C(41)	104.4(1)
Ru(1)−P(1)−C(11)	124.1(1)	P(1)−C(1)−C(2)	115.1(3)
C(1)−P(1)−C(5)	103.9(2)	C(1)−C(2)−C(3)	115.4(3)
C(1)−P(1)−C(11)	101.6(2)	C(2)−C(3)−C(4)	116.6(3)
C(5)−P(1)−C(11)	103.3(2)	P(2)−C(4)−C(3)	114.6(2)

Results and Discussion

Earlier attempts to grow X-ray diffraction quality crystals of $RuCl_2(dppb)(PPh_3)$ (**4**) were unsuccessful. Therefore, a comparative solid-state ^{31}P NMR spectroscopic study of **4** and $RuCl_2(PPh_3)_3$ (**1**) was undertaken in the hope of determining the solid-state structure of **4**. Complex **1** was chosen for comparison as the structure had previously been elucidated by X-ray studies.[17] Eventually X-ray quality crystals of **4** were grown, as were crystals of $RuBr_2(PPh_3)_3$ (**2**), and diffraction studies of the two complexes allowed comparison with the solid-state structure of **1** and the evaluation of solid-state NMR (^{31}P CP/MAS) as a method for solid-state structural characterization.

Molecular Structures. The molecular structure of **2** (Figure 1) is crystallographically isomorphous to that determined previously by La Placa and Ibers[17] for the chloro analog $RuCl_2$-$(PPh_3)_3$ (**1**). The geometry of **2** at the Ru is distorted square

(14) teXsan: Crystal Structure Analysis Package (1985, 1992), Molecular Structure Corp., The Woodlands, TX.

(15) *International Tables for X-ray Crystallography*; Kynoch Press: Birmingham, England, 1974; Vol. IV, pp 99−102.

(16) *International Tables for X-ray Crystallography*; Kluwer Academic Publishers: Boston, MA, 1992; Vol. C, pp 200−206.

(17) La Placa, S. J.; Ibers, J. A. *Inorg. Chem.* **1965**, *4*, 778.

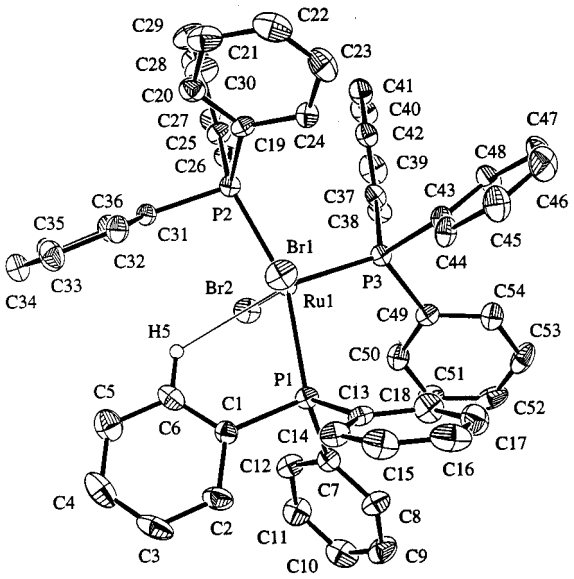

Figure 1. ORTEP plot of $RuBr_2(PPh_3)_3$ (**2**). Thermal ellipsoids for non-hydrogen atoms are drawn at 33% probability.

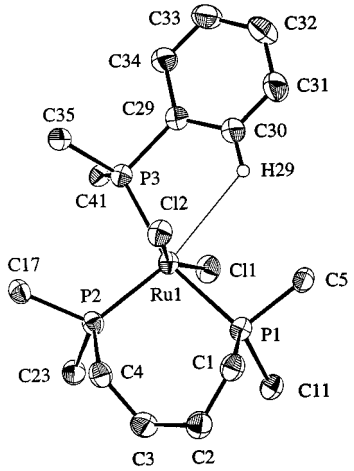

Figure 2. ORTEP plot $RuCl_2(dppb)(PPh_3)$ (**4**). Thermal ellipsoids for non-hydrogen atoms are drawn at 33% probability (some of the phenyl carbons have been omitted for clarity).

pyramidal, with the sixth coordination site blocked by an *ortho*-H (H(5)) of a PPh_3 ligand. The Ru(1)−H(5) distance, 2.68 Å, compares with the 2.59 Å observed for the metal−*ortho*-H distance in **1**.[17]

The geometry of **4** is essentially identical to that of **1** and **2** (Figure 2). The Ru(1)−H(29) distance is 2.69 Å, essentially identical to the corresponding distance observed in **2**. The metal centers of **2** and **4** are best described as being near the center of gravity of a distorted square pyramid composed of *trans* P atoms and *trans* Cl atoms in the base, with a third P atom at the apex. The main differences in the structures of **1**, **2**, and **4** are probably due to the chelating dppb ligand in **4**. For example, the P−Ru−P angle for the dppb chelate in **4** is 97.01°, while the corresponding P−Ru−P angles in **1** and **2** are 101.1 and 101.50°, respectively.

The Ru metal center in each of **1**, **2**, and **4** is found above the mean plane created by the two halides and two basal phosphorus atoms, the Ru atom being observed 0.456,[17] 0.518, and 0.404 Å above the basal plane, respectively. In all three complexes, the apical Ru−P distances (2.20−2.23 Å) are shorter than the basal Ru−P distances (2.34−2.42 Å). Also, the Ru−P distances of the phosphine groups involved in the agostic hydrogen interaction (i.e., the *ortho*-H of a phenyl group) are longer than the other basal Ru−P bond lengths.

Of note is the Ru−P(1)−C(1) (the *ipso* carbon of the phenyl group involved in the agostic interaction) bond angle in **2** of 104.4° which is significantly smaller than the other Ru−P−C(*ipso*) angles (which range from 114−129°) with the exception of that involving one of the phenyl rings attached to the other basal P-atom on the "open side" of the molecule (Ru−P(2)−C(31) = 100.1°). This is also observed in **4** where the Ru−P−C(*ipso*) angles on the open side of the complex are 105.3° for the phenyl group (C(29)) involved in the agostic interaction and 101.3° for a phenyl group (C(5)) on the other basal P(1) atom. These smaller *ipso* angles are thought to result from the mutual interaction of the phenyl groups, this being reflected in the larger Ru−P−C(*ipso*) angles of 128.5 and 128.9° in **2** for C(7) and C(25), respectively: the phenyl groups seem to be effectively "pushed back" from the apex of the square pyramid toward the open side of the complex. The geometry of **4** is somewhat less sterically demanding than in **2** as the number of phenyl groups is decreased by replacing two PPh_3 ligands with dppb; this is reflected in the Ru−P−C(*ipso*) angles being somewhat less extreme in **4** compared with those in **2** (see Table 2).

Other five-coordinate Ru(II) phosphine complexes that have been characterized by X-ray crystallography include $RuCl_2(PMA)(P(p\text{-tolyl})_3)$[18] and $RuCl_2(isoPFA)(PPh_3)$[19] which both contain P−N chelates (PMA = *o*-(diphenylphosphino)-*N*,*N*-dimethylaniline and isoPFA = 1-[α,α-dimethylethyl]-2-(diisopropylphosphino)ferrocene). Interestingly, the latter complex has an *ortho*-H of a PPh_3 ligand blocking the sixth coordination site of an octahedron while the former complex does not. $RuCl_2(PMA)(P(p\text{-tolyl})_3)$ is known to coordinate a range of small molecules including O_2, CO, H_2O, H_2S, SO_2, and MeOH.[18]

The mixed-phosphine complexes $RuCl_2(dppb)(P(p\text{-tolyl})_3)$ (**5**), $RuBr_2(dppb)(PPh_3)$ (**6**), and the previously reported $RuCl_2$-((*R*)-binap)(PPh_3)[2,20] are all believed to have the same geometry around Ru as in **4**, on the basis of low-temperature $^{31}P\{^1H\}$ NMR spectroscopic studies (Table 3).

The observed ABX pattern is consistent with the structure determined by X-ray crystallography and ^{31}P CP/MAS NMR spectroscopy for **4**. The spectra are consistent with two *cis*- and one *trans*-phosphorus−phosphorus interactions, the *trans* $^2J_{PP}$ coupling constants being much greater in magnitude than *cis* $^2J_{PP}$ coupling constants.[22]

The dynamic process observed in the room temperature $^{31}P\{^1H\}$ NMR spectrum of **5** (and the other mixed-phosphine complexes) (Table 3) is due to intramolecular exchange of the dppb (or binap)[2,20,23] nuclei on the NMR time scale as observed for **4** by Jung et al.[7] The rate of PPh_3 dissociation is too slow to be responsible for the fluxional process observed at room temperature (the line width of the PPh_3 was essentially invariant over the temperature range −66 to +20 °C).

^{31}P CP/MAS NMR Spectroscopy. The ^{31}P CP/MAS NMR spectra of $RuCl_2(PPh_3)_3$ (**1**) and $RuCl_2(dppb)(PPh_3)$ (**4**) both show the isotropic peaks as well as peaks at integral values of the spinning frequency (i.e., spinning sidebands). Figures 3 and

(18) Mudalige, D. C.; Rettig, S. J.; James, B. R.; Cullen, W. R. *J. Chem. Soc., Chem. Commun.* **1993**, 830.
(19) Hampton, C. R. S. M.; Butler, I. R.; Cullen, W. R.; James, B. R.; Charland, J.-P.; Simpson, J. *Inorg. Chem.* **1992**, *31*, 5509.
(20) Mezzetti, A.; Costella, L.; Del Zotto, A.; Rigo, P.; Consiglio, G. *Gazz. Chim. Ital.* **1993**, *123*, 155.
(21) Hoffman, P. R.; Caulton, K. G. *J. Am. Chem. Soc.* **1975**, *97*, 4221.
(22) Dixon, K. R. In *Multinuclear NMR*; Mason, J., Ed.; Plenum: New York, 1987; Chapter 13.
(23) Joshi, A. M. Ph.D. Thesis, The University of British Columbia, 1990.

Table 3. $^{31}P\{^1H\}$ NMR Data for $RuCl_2(PPh_3)_3$ and $RuX_2(dppb)(PAr_3)$ Complexes

complex	solvent	temp (°C)	chem shift, δ	$^2J_{PP}$, Hz
$RuCl_2(PPh_3)_3$ (**1**)[a]	CD_2Cl_2	−97	$\delta_A = 75.7$	$^2J_{AX} = 30.5$
			$\delta_X = 24.1$	
$RuCl_2$(dppb)(PPh_3) (**4**)	C_6D_6	20	$\delta_A = 25.7$	140[b]
	C_7D_8	20	$\delta_A = 26.7$	142[b]
	C_7D_8	−70	$\delta_A = 28.4$	$^2J_{AX}$ = unresolved
			$\delta_B = 36.2$	$^2J_{BX} = -37.7$
			$\delta_X = 86.1$	$^2J_{AB} = 297.5$
	CH_2Cl_2[c]	−75	$\delta_A = 26.3$	$^2J_{AX} = -22.6$
			$\delta_B = 35.2$	$^2J_{BX} = -37.5$
			$\delta_X = 83.2$	$^2J_{AB} = 302.4$
$RuCl_2$(dppb)(P(*p*-tolyl)$_3$) (**5**)	C_6D_6	20	$\delta_A = 25.5$	141[b]
	CD_2Cl_2	20	$\delta_A = 24.5$	141[b]
	CD_2Cl_2	−66	$\delta_A = 25.9$	$^2J_{AX}$ = unresolved
			$\delta_B = 36.6$	$^2J_{BX} = -35.7$
			$\delta_X = 83.9$	$^2J_{AB} = 303.2$
	$CDCl_3$	−58	$\delta_A = 24.7$	$^2J_{AX}$ = unresolved
			$\delta_B = 34.9$	$^2J_{BX} = -35.9$
			$\delta_X = 84.4$	$^2J_{AB} = 303.7$
$RuBr_2$(dppb)(PPh_3) (**6**)	C_6D_6	20	$\delta_A = 27.6$	135[b]
	CD_2Cl_2	20	$\delta_A = 27.3$	145[b]
	CD_2Cl_2	−66	$\delta_A = 29.3$	$^2J_{AX}$ = unresolved
			$\delta_B = 37.5$	$^2J_{BX} = -35.8$
			$\delta_X = 86.8$	$^2J_{AB} = 300.4$

[a] Data taken from ref 21. [b] Tripletlike pattern; *J* value indicates line spacing. The δ_B of the AB_2 pattern observed at 20 °C appears as a very broad resonance between 50−60 in all cases. [c] Data taken from ref 7.

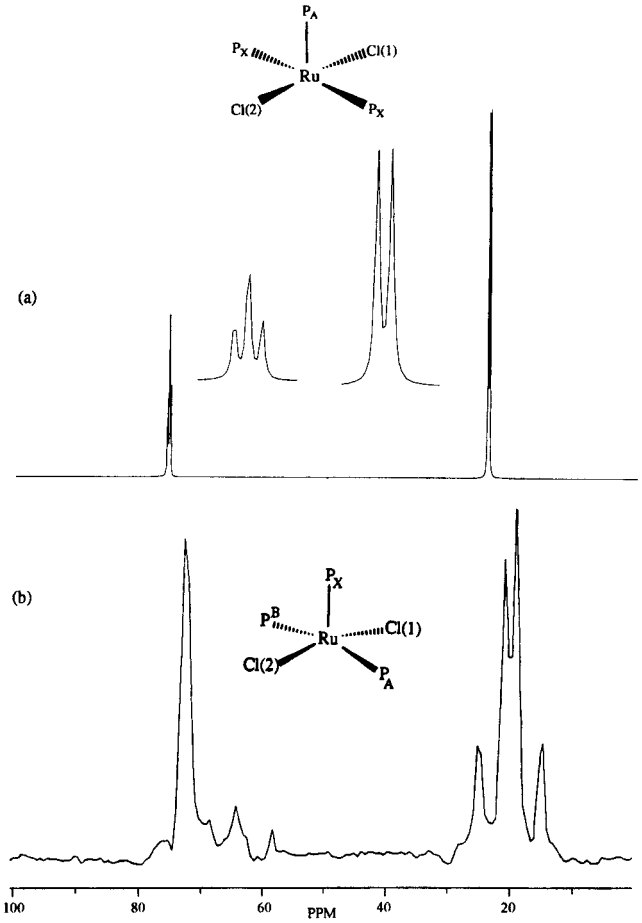

Figure 3. (a) Simulated solution NMR spectrum of $RuCl_2(PPh_3)_3$ (**1**) obtained using the literature data,[21] with the expansion shown inset. (b) 80.99 MHz ^{31}P CP/MAS NMR (*TOSS*) spectrum of **1**.

4 show simulated solution ^{31}P, and ^{31}P CP/MAS (*TOSS* = TOtal Suppression of Sidebands)[24] NMR spectra of **1** and **4**, respectively. Table 3 lists the low-temperature $^{31}P\{^1H\}$ NMR solution data used for the simulations illustrated in Figures 3 and 4, as well as for **5** and **6**; Table 4 lists the ^{31}P CP/MAS NMR data for **1** and **4**.

The two mutually *trans* basal PPh_3 ligands in **1** are equivalent in solution even at −97 °C as evidenced by the AX_2 pattern simulated in Figure 3a. However, in the solid state the two basal P-atoms are inequivalent as evidenced by both the ABX pattern observed in the ^{31}P CP/MAS (*TOSS*) NMR spectrum (Figure 3b) and the X-ray diffraction study performed by La Placa and Ibers,[17] one of the basal PPh_3 ligands showing a weak interaction between the Ru center and an *ortho*-phenyl hydrogen; the $^2J_{AB}$ scalar coupling is 333 Hz for the *trans*-disposed phosphines.

The move of the solid-state chemical shifts to higher field relative to the solution values implies increased shielding in the solid state, particularly for the resonance at 16.9 ppm designated as δ_A. Such chemical shift differences between the solid-state CP/MAS and solution NMR data have been observed for other compounds, including tertiary phosphines and their transition metal complexes.[25−32] Differences of ≤ 5−6 ppm are common, and the compounds are still considered to possess similar structures in solution and in the solid state, at least qualitatively.[25−32] Larger chemical shift differences are often considered a manifestation of major structural differences.[26] The highest-field signal observed at δ 16.9 in the ^{31}P CP/MAS NMR spectrum of **1** is attributed to the basal PPh_3 with a longer Ru−P bond (2.412 Å[17]). The other upfield resonance of **1** at δ 22.8 corresponds to the basal P atom that is not involved in the *ortho*-phenyl hydrogen−Ru interaction (the Ru−P bond length is

(24) Dixon, W. T.; Schaefer, J.; Sefcik, M. D.; Stejskal, E. O.; McKay, R. A. *J. Magn. Reson.* **1982**, *49*, 341.
(25) Diesveld, G. E.; Menger, E. M.; Edzes, H. T.; Veeman, W. S. *J. Am. Chem. Soc.* **1980**, *102*, 7935.
(26) Maciel, G. E.; O'Donnel, D. J.; Greaves, R. *Adv. Chem. Ser.* **1982**, *196*, 389.
(27) Bemi, L.; Clark, H. C.; Davies, J. A.; Fyfe, C. A.; Wasylishen, R. E. *J. Am. Chem. Soc.* **1982**, *104*, 438.
(28) Bemi, L.; Clark, H. C.; Davies, J. A.; Drexler, D.; Fyfe, C. A.; Wasylishen, R. E. *J. Organomet.Chem.* **1982**, *224*, C5.
(29) Clark, H. C.; Davies, J. A.; Fyfe, C. A.; Hayes, P. J.; Wasylishen, R. E. *Organometallics* **1983**, *2*, 177.
(30) Fyfe, C. A.; Clark, H. C.; Davies, J. A.; Hayes, P. J.; Wasylishen, R. E. *J. Am. Chem. Soc.* **1983**, *105*, 6577.
(31) Kroto, H. W.; Klein, S. I.; Meidine, M. F.; Nixon, J. F.; Harris, R. K.; Packer, K. J.; Reams, P. *J. Organomet. Chem.* **1985**, *280*, 281.
(32) Komoroski, R. A.; Magistro, A. J.; Nicholas, P. P. *Inorg. Chem.* **1986**, *25*, 3917.

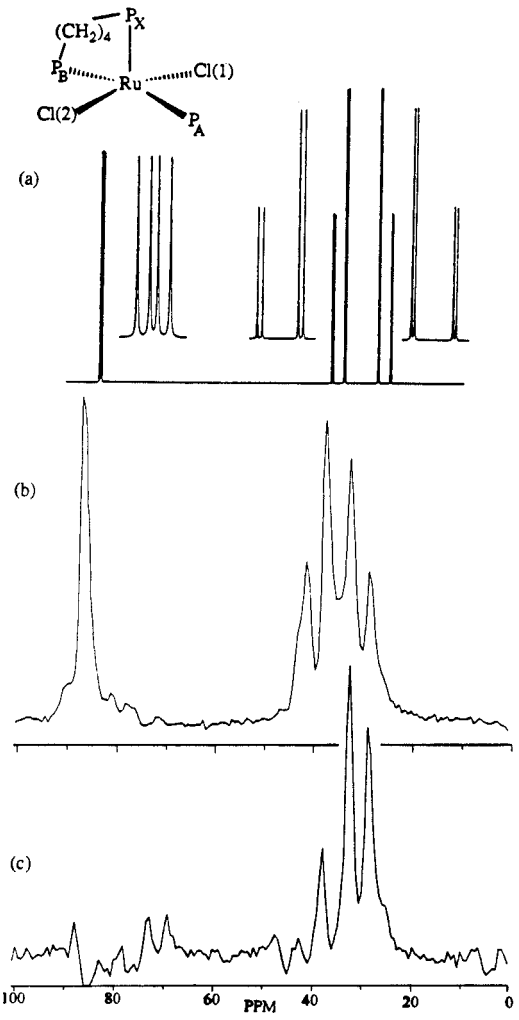

Figure 4. (a) Simulated solution NMR spectrum of $RuCl_2(dppb)(PPh_3)$ (**4**) obtained using the literature data,[7] with the expansion shown inset. (b) 80.99 MHz ^{31}P CP/MAS NMR (*TOSS*) spectrum of **4**. (c) Spectrum as in (b) but showing nonquaternary suppression (NQS) with a dipolar dephasing of 303 μs.

Table 4. Solid-State ^{31}P CP/MAS NMR Spectral Data for $RuCl_2(PPh_3)_3$ (**1**) and $RuCl_2(dppb)(PPh_3)$ (**4**)

complex	chem shift, δ (assgnt) ($^2J_{PP}$, Hz)		
$RuCl_2(PPh_3)_3$ (**1**) (ABX pattern)	16.9 (P_A)	22.8 (P_B) ($^2J_{AB} = 333$)	72.5 (P_X)
$RuCl_2(dppb)(PPh_3)$ (**4**) (ABX pattern)	30.4 (P_A)	39.2 (P_B) ($^2J_{AB} = 320$)	86.3 (P_x)

2.374 Å[17]). These assignments are based on an established empirical linear correlation between the crystallographically determined Ru−P distances in a series of Ru(II)−PPh_3 complexes and the corresponding ^{31}P chemical shifts observed in solution, the chemical shifts becoming more high field with increasing Ru−P bond lengths.[33] This trend in ^{31}P chemical shift with Ru−P bond length has also been observed for Ru(II)−dppb complexes.[34] Of note, the negative slope (-2.91×10^{-3} Å ppm^{-1}) for the graph of Ru−P bond length versus ^{31}P chemical shift for the Ru(II)−dppb complexes[34] is identical to that of the plot for the PPh_3 systems;[33] however, the intercepts are somewhat different (2.423 Å for the dppb systems and 2.465 Å for the PPh_3 systems). The difference of 52.7 ppm between the apical and the averaged basal phosphorus chemical shifts in the ^{31}P CP/MAS NMR spectrum is close to the 51.6 ppm difference observed in the solution spectrum.

The solid-state ^{31}P CP/MAS (*TOSS*) NMR spectrum of $RuCl_2(dppb)(PPh_3)$ (**4**) exhibits an ABX pattern similar to that observed in the low-temperature solution NMR spectrum (see Figure 4). The solid-state chemical shifts correspond well with the solution parameters (Tables 3 and 4). The shift of ~3−4 ppm in the CP/MAS NMR resonances toward lower field relative to the solution values indicates reduced shielding of the P nuclei in the solid state, opposite to the behavior observed for $RuCl_2(PPh_3)_3$; see above (Tables 3 and 4). The high field AB quartet centered at δ 34.8 with a $^2J_{AB}$ scalar coupling 320 Hz again indicates *trans*-disposed inequivalent phosphines. This 320 Hz value is somewhat greater than the corresponding solution phase coupling of 302.4 Hz, suggesting the presence of additional constraints and interactions in the solid state which may not exist, or are averaged out, in solution. The downfield signal at δ 86.3 is assigned to an apical P atom and, because of the forced *cis* configuration of the chelating dppb ligand, the apical phosphine must be part of the diphosphine. Again, the *cis* P−Ru−P couplings, $^2J_{AX}$ and $^2J_{BX}$, cannot be seen in the CP/MAS NMR spectrum because their magnitudes are much smaller than the typical line widths encountered in solid-state NMR spectra ($\omega_{1/2} \sim 50-100$ Hz).

The resonances at 30.4 (δ_A) and 39.2 (δ_B) are assigned to the PPh_3 ligand and the basal $-PPh_2$ part of the dppb chelate, respectively, on the basis of the results of a nonquaternary suppression (NQS) experiment,[35] in which only the peaks due to P atoms attached to a nonquaternary carbon are suppressed (presumably because of relatively fast relaxation of the P nucleus by the protons on the nonquaternary carbon). The NQS spectrum in Figure 4 shows considerable loss of intensity for the resonances at δ 86.3 and 39.2, the signals which are due to P nuclei attached to a nonquaternary carbon (i.e., the alkyl chain of dppb). The unaffected resonance at δ 30.4 is therefore assigned to the PPh_3 ligand containing three P-phenyl (quaternary carbon) linkages. The similarities between the solution and the solid-state NMR data for $RuCl_2(dppb)(PPh_3)$ suggest very similar solution (at least at low temperature) and solid-state structures.

Recently, $^1J(^{101,99}Ru,^{31}P)$ coupling in ^{31}P CP/MAS spectra of Ru/phosphorus-containing complexes has been observed with $^1J(^{99}Ru,^{31}P)$ values ranging from 100 to 174 Hz for the Ru−phosphine and −phosphido interactions.[36] No P−Ru coupling was observed in the ^{31}P CP/MAS NMR spectrum in the present study, although the downfield signal in Figure 4b does show an approximate six-line satellite as expected for coupling to a nucleus of spin $I = {}^5/_2$ (i.e., $^{101,99}Ru$); however, closer inspection suggests that the lines are due to incomplete suppression of spinning sidebands which coincidentally at this spinning rate (3.5 kHz) superimpose on the downfield signal.

Reactivity of $RuCl_2(dppb)(PPh_3)$ and the Preparation of $(P-P)Cl_2Ru(\mu_2\text{-}P-P)RuCl_2(P-P)$ Complexes. The reactivity of the five-coordinate mixed-phosphine complexes with neutral two-electron donor ligands was investigated in attempts to isolate Ru(II) complexes containing a single dppb ligand per Ru. It is desirable to remove the PPh_3 ligand from the Ru(II) complexes for their potential use as hydrogenation catalysts, because work from this laboratory on imine hydrogenation has shown $RuCl_2(P-P)(PPh_3)$ species to be relatively poor catalysts compared

(33) Jessop, P. G.; Rettig, S. J.; Lee, C.-L.; James, B. R. *Inorg. Chem.* **1991**, *30*, 4617.
(34) MacFarlane, K. S. Ph.D. Thesis, The University of British Columbia, 1995.
(35) Opella, S. J.; Frey, M. H. *J. Am. Chem. Soc.* **1979**, *101*, 5854.
(36) Eichele, K.; Wasylishen, R. E.; Corrigan, J. F.; Doherty, S.; Sun, Y.; Carty, A. J. *Inorg. Chem.* **1993**, *32*, 121.

Table 5. $^{31}P\{^1H\}$ NMR Data (121.42 MHz, 20 °C) for the Dinuclear Complexes $[(L)(dppb)Ru(\mu\text{-}Cl)_3RuCl(dppb)]$

complex	solvent	chem shift, δ	$^2J_{PP}$, Hz
dmso, Me_2SO[a] (**8**)	$CDCl_3$	$\delta_A = 54.2$, $\delta_B = 51.2$	42.8
		$\delta_C = 42.2$, $\delta_D = 29.5$	30.2
	C_6D_6	$\delta_A = 53.9$, $\delta_B = 52.9$	43.8
		$\delta_C = 42.5$, $\delta_D = 33.7$	29.6
tmso, C_4H_8SO (**9**)	$CDCl_3$	$\delta_A = 54.7$, $\delta_B = 50.8$	41.1
		$\delta_C = 43.4$, $\delta_D = 26.3$	27.8
	C_6D_6	$\delta_A = 55.1$, $\delta_B = 52.2$	42.8
		$\delta_C = 44.2$, $\delta_D = 29.1$	29.0
L = dms, Me_2S (**10**)	$CDCl_3$	$\delta_{A,B} = 51.3$[b]	
		$\delta_C = 48.2$, $\delta_D = 46.0$	35.6
	C_6D_6	$\delta_A = 52.5$, $\delta_B = 51.8$	44.1
		$\delta_C = 48.6$, $\delta_D = 46.2$	35.3
tht, C_4H_8S (**11**)	$CDCl_3$	$\delta_A = 51.9$, $\delta_B = 51.2$	43.2
		$\delta_C = 49.1$, $\delta_D = 46.7$	36.1
	C_6D_6	$\delta_{A,B} = 52.3$[a]	
		$\delta_C = 49.5$, $\delta_D = 47.1$	36.1

[a] The chemical shifts differ slightly from those given in the literature[2] because of the differences in the methods of referencing. [b] Indicates unresolved AB pattern.

with $Ru_2Cl_4(P-P)_2$ complexes.[1] Recall that, in solution, the mixed-phosphine complexes $RuCl_2(P-P)(PPh_3)$ are in equilibrium with the dinuclear $Ru_2Cl_4(P-P)_2$ species (see eq 1).

Occasionally, in the preparation of **4** or **5**, a bridged-phosphine side product $(dppb)Cl_2Ru(\mu_2\text{-}dppb)RuCl_2(dppb)$ is isolated.[2,7] This species can be prepared in good yields by addition of 2 equiv of dppb to $RuCl_2(PPh_3)_3$ (**1**).[37] Although the phosphine-bridged, bromo-analog $(dppb)Br_2Ru(\mu_2\text{-}dppb)RuBr_2(dppb)$ was not observed as a side product in the preparation of **6**, it was isolated in this work by the addition of 2 equiv of dppb to **2**. The complex **7a** has properties similar to those of the previously reported chloro analog,[37] being essentially insoluble in most nonaromatic solvents and only sparingly soluble in aromatic solvents. Also prepared by the same method is $(dcypb)Cl_2Ru(\mu_2\text{-}dcypb)RuCl_2(dcypb)$ (**7b**). The mixed-phosphine complex $RuCl_2(dcypb)(PPh_3)$ has been observed in solution [−70 °C, CD_2Cl_2, $\delta_A = 17.1$, $\delta_B = 24.1$, $\delta_X = 88.0$; $^2J_{AB} = 303.7$, $^2J_{AX}$ and $^2J_{BX}$ are unresolved] but has not yet been isolated as it is very soluble in most common organic solvents. Despite the insolubility of the bridged-phosphine complexes, they still can be useful as starting materials (e.g., for synthesis of $RuCl_2(dppb)(py)_2$ (py = pyridine[38]). The corresponding bridged (*R*)-binap (2,2′-bis(diphenylphosphino)-1,1′-binaphthyl) analog could not be prepared by addition of 2 equiv of the diphosphine to $RuCl_2(PPh_3)_3$ as used to prepare **7a,b**. The binap ligand is presumably too rigid to effectively bridge two metals.

Work from this laboratory has previously reported on the preparation from $RuCl_2(dppb)(PPh_3)$ of the complexes $Ru_2Cl_4(dppb)_2(L)$, where L = CO,[2] NEt_3,[2] MeCN,[39] and $PhCH_2NH_2$,[40] while $Ru_2Cl_4(dppb)_2(dmso)$ (**8**) was prepared from *cis*-$RuCl_2(dmso)_4$.[2] Other dinuclear $Ru_2Cl_4(dppb)_2(L)$ species (L = η^2-H_2, N_2, and Me_2CO) were prepared directly from the air-sensitive dimer $[RuCl(dppb)]_2(\mu\text{-}Cl)_2$.[2]

The reactions of dmso, tmso, dms, and tht with **4** have now been found to give the corresponding $Ru_2Cl_4(dppb)_2(L)$ species **8**−**11** in high yield. This route to **8** is cleaner than the original route from *cis*-$RuCl_2(dmso)_4$, which required removal of the side products, $[RuCl(dppb)]_2(\mu\text{-}Cl)_2$ and $Ru_2Cl_4(dppb)_3$, before isolation of the product;[2] the *S*-bonded dmso, indicated by the ν_{SO} value, was confirmed by an X-ray study.[2] Complex **8** was not formed by reacting $Ru_2Cl_4(dppb)_3$ with excess dmso.

The $Ru_2Cl_4(dppb)_2(L)$ species, where L = dmso, tmso, dms, or tht, have structure **I** as evidenced by $^{31}P\{^1H\}$ NMR

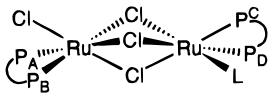

I

spectroscopy (Table 5). Each of the complexes **8**−**11** shows spectra consisting of two independent AB patterns of equal integral intensity as observed previously for other triply-chloro-bridged diruthenium complexes.[2] Of the two AB quartet patterns, the relatively downfield pattern is insensitive to the nature of ligand L ($\delta_{AB} = 52 \pm 2$, $^2J_{AB} = 43 \pm 2$ Hz) and is therefore assigned as shown to the $(\mu\text{-}Cl)_3RuCl(P-P)$ portion of the molecule; the other set of signals varies with the nature of L ($\delta_{CD} = 26-49$, $^2J_{CD} = 28-36$ Hz) and is attributed to the L(P−P)Ru fragment. Occasionally, one of the two AB quartets (the δ_{AB} end) is not resolved in a certain solvent and appears as a broad singlet, as for **10** in $CDCl_3$ and **11** in C_6D_6, the spectra showing strong second-order effects (see Table 5). The greater difference in the chemical shift between the two halves of the AB pattern in C_6D_6 (**10**) or $CDCl_3$ (**11**) may prevent averaging of the signals. It is worth noting that the spectra of complexes **10** and **11** are resolved in "opposite" solvents. The second-order effects have been previously observed for $Ru_2Cl_4(dppb)_2(PhCN)$ in CD_2Cl_2; if the solution of the nitrile complex is cooled to −40 °C, the singlet observed in the $^{31}P\{^1H\}$ NMR spectrum at rt begins to resolve into a tight AB pattern.[40]

The IR spectrum of **9** shows $\nu_{S=O}$ at 1093 cm^{-1} indicating that the coordinated tmso is *S*-bonded as previously confirmed for **8** by X-ray crystallography.[2]

Conclusions. This study has demonstrated the utility of ^{31}P CP/MAS NMR spectroscopy in determining the geometry and structure of Ru(II) phosphine complexes, and the solid-state structure suggested by ^{31}P CP/MAS NMR was confirmed by X-ray crystallography in the case of $RuCl_2(dppb)(PPh_3)$. ^{31}P CP/MAS NMR spectroscopy offers an obvious advantage over solution ^{31}P NMR spectroscopy where the spectra can sometimes be complicated by exchange processes. The utility of the complex $RuCl_2(dppb)(PPh_3)$ as a precursor for the preparation of $[(L)(dppb)Ru(\mu\text{-}Cl)_3RuCl(dppb)]$ species is further established.

Acknowledgment. We thank the Natural Sciences and Engineering Research Council of Canada for financial support, Johnson Matthey Ltd. and Colonial Metals Inc. for the generous loan of $RuCl_3 \cdot xH_2O$, and Dr. A. Root for experimental assistance in performing the solid-state ^{31}P CP/MAS NMR spectroscopic experiments.

Supporting Information Available: Tables of atomic coordinates and equivalent isotropic thermal parameters, hydrogen atom parameters, anisotropic thermal parameters, complete bond lengths and angles, and torsion angles for the structures of **2** and **4** (40 pages). Ordering information is given on any current masthead page.

IC960860+

(37) (a) Bressan, M.; Rigo, P. *Inorg. Chem.* **1975**, *14*, 2286. (b) James, B. R.; McMillan, R. S.; Morris, R. H.; Wang, D. K. W. *Adv. Chem. Ser.* **1978**, *167*, 123.
(38) Batista, A. A.; Queiroz, S. L.; Oliva, G.; Gambardella, M. T. do. P.; Santos, R. H. A. Personal communication.
(39) Fogg, D. E.; James, B. R. *Inorg. Chem.*, submitted for publication.
(40) Fogg, D. E.; James, B. R. *Inorg. Chem.* **1995**, *34*, 2557.